### ZERO- REINFORCEMENT VESSEL CLOSURES

#### Grant McClellan

Nuclear Engineering
Babcock & Wilcox, A McDermott Company
Cambridge, Ontario
Canada

#### Yanghu Mou

Nuclear Engineering
Babcock & Wilcox, A McDermott Company
Cambridge, Ontario
Canada

#### **ABSTRACT**

Access to the secondary side of a Nuclear Steam Generator is required in order to properly inspect and maintain critical components throughout the life. For the most part, it is only on newer units that sufficient openings have been provided. Older units must be field modified to provide access to the tube bundle and internal lateral support components for inspection and penetration by cleaning equipment. In order to avoid post weld heat treatment after welding on some materials it would be desirable to machine the opening directly into the pressure boundary without providing weld build-up to compensate for the material removed. In such a case, the pressure boundary may be locally thinned below the minimum thickness required by the ASME Code. As a result it is not possible to meet reinforcement limits or elastic primary stress limits of the Code. However, the ASME Code permits justification of the design by utilizing elastic-plastic methods.

Elastic-plastic analysis can be utilized to demonstrate shakedown to elastic action and to demonstrate that small deformations in the region of the gasket seating surfaces, or any loss of bolt preload, have not compromised leak tightness. Employing the technique developed by the authors for application in ANSYS, it is feasible to carry-out such a design analysis including the effects of time varying thermal stress. This paper presents the highlights of such an analysis. It is important to note that the method also permits the analysis of openings in locations formerly considered too restrictive, such as near supports and major structural discontinuities.

#### 1.0 INTRODUCTION

Advances in computer software and hardware now make it feasible to carry out analyses that not too long ago would have been considered far too computing intensive and prohibitive from both a schedule and cost point of view. This computing power can be employed to design openings that formerly were considered unacceptable because of the proximity of attachments and structural discontinuities and the available shell thickness. Figure 1.0-1 shows an example of such an opening design. If an opening is placed in a shell whose thickness is the ASME Code minimum thickness, no reinforcement is available to compensate for material removed. In addition, elastic analysis primary stress limits cannot be satisfied in such a case. Elastic-plastic analysis can, however, be employed to justify the design. In this paper a zero-reinforcement closure is analyzed for warmup/rapid cooldown transient. Analysis for the combined effect of thermal transient and pressure loading is carried out in "real-time" in order to account for the accumulation of inelastic strains and to explore closure shake-down.

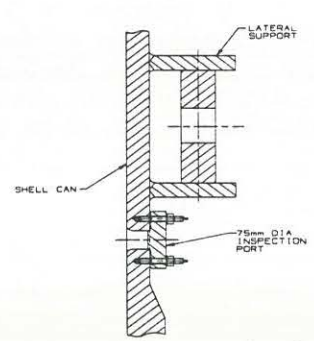


Figure 1.0-1: Zero-reinforcement Opening Example

If a design can be shown to shake-down to elastic action, after a few load cycles employing elastic-plastic analysis, subsequent fatigue analysis can be carried out on an elastic basis. Elastic-plastic analysis can also be utilized to demonstrate that small deformations in the region of the gasket seating surfaces or any loss of bolt preload have not compromised leak tightness.

## 2.0 ZERO REINFORCEMENT ACCESS OPENING DESIGN

An access opening in a secondary side shell of a nuclear steam generator is shown in *Figure* 2.0-1. The opening is in a portion of the secondary shell that is at the minimum ASME thickness. The design employs no weld build-up and is installed in the field by machining a flat for the gasket contact surface directly into the shell. According to the reinforcement rules (NB-3332), an opening does not require reinforcement if it satisfies the following inequality, (Ref. 1):

$$0.2\sqrt{Rt} > D$$

Larger openings would have to satisfy the primary local stress limit or be reinforced. It can be shown that if a cylindrical shell containing an opening greater in size than that limited by NB-3332 is stressed to its general primary stress limit it will fail the  $P_L$  stress limit. However a detailed elastic-plastic analysis to NB-3228.3 can be employed to justify the design.

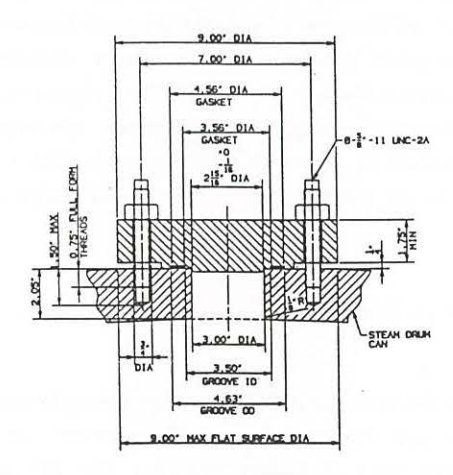


Figure 2.0-1: Zero-Reinforcement Vessel Closure

# 3.0 WARMUP START-UP/RAPID COOLDOWN TRANSIENT LOADING

The following transient loading was considered in the analysis.

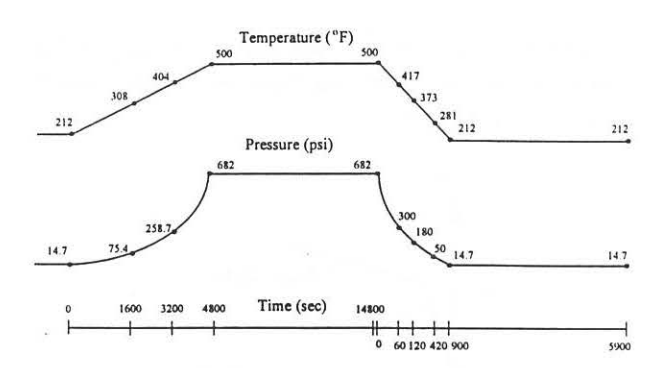


Figure 3.0-1: Warmup/Rapid Cooldown Transients

#### 4.0 ACCEPTANCE CRITERIA OF THE DESIGN

The acceptance criteria included consideration of: ① accumulated deformations in order to preclude loss of the bolt preload; ② the difference in the outward displacement between the points on the surface of the shell in order to preclude 'bell-mouthing'. This accumulated displacement (distortion) should also be small and asymmptotic after several load cycles. This requirement will ensure that shakedown of the structure occurs and collapse is precluded; ③ changes in contact pressure between the cover and the shell to evaluate potential adverse effects on leak tightness of the joint.

#### 5.0 FINITE ELEMENT MODEL

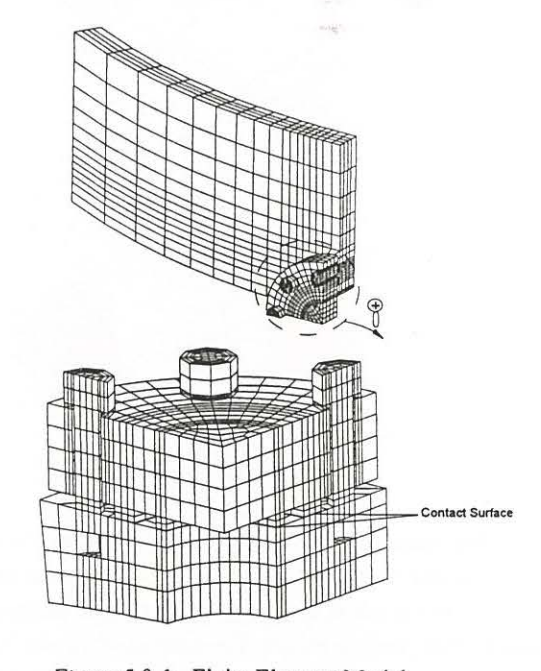
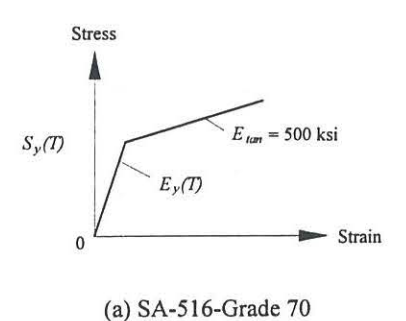


Figure 5.0-1: Finite Element Model

All modeling and analysis was carried out using ANSYS version 5.2. *Figure* 5.0-1 shows the finite element model used for the elastic-plastic analysis.



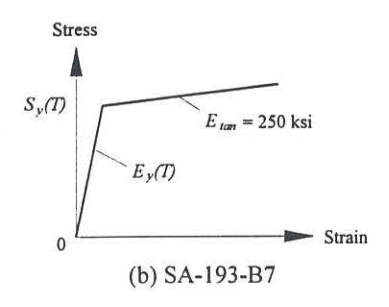


Figure 5.0-2: Stress-strain Curve

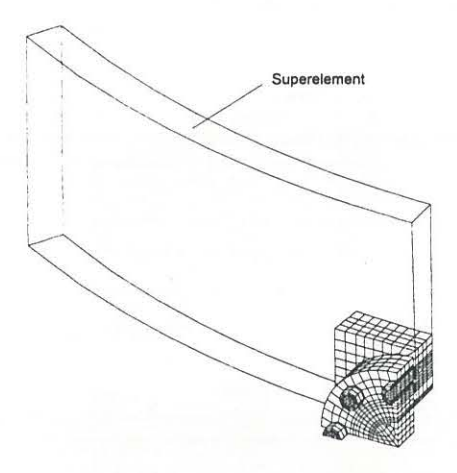


Figure 5.0-3: Superelement

The material of the cover is the same as the shell. The material nonlinearity of both the cover and the shell are modeled as bilinear kinematic hardening. Bolt stress is checked to assure that no bolt yielding occurs. The material of the shell is SA-516-Grade 70 and the material of the bolt is SA-193-B7. *Figure* 5.0-2 shows the representation of the true stress-strain curves of the

materials, where  $S_{y}(T)$  and  $E_{y}(T)$  are the yield stress and elastic modulus which are functions of temperature.

Substructuring was employed to condense a group of finite elements into one element which is called a superelement. The size and extent of the region to be modeled as a superelement was determined by elastic analysis (see *Figure* 5.0-3).

# 6.0 THERMAL TRANSIENT AND CYCLIC LOADING FOR FINITE ELEMENT ANALYSIS

The warmup start-up/rapid cooldown transient process on the secondary side of the steam generator as depicted in Figure 3.0-1 is applied to all internal surfaces of a thermal finite element model. Theoretically, the temperatures at each particular load substep should be read into the structural model. This is impractical due to disk space limit and execution time. A means has been developed to virtually eliminate the I/O portion of the execution time so that the execution time is approximately the same as that of a pressure load case. The scheme is based on the simple observation that the temperature differences within the geometry are the cause of thermally induced stress and strain.

If the temperature differences between key node pairs within the geometry are plotted as a function of time, smooth curves interrupted by occasional abrupt changes in slope are evident. It is possible to visualize the same curves being represented quite accurately by piece-wise continuous straight line curve fits. This idea is illustrated in *Figure* 6.0-1 in which the time points were picked such that the connection of the corresponding temperature distribution points (Fundamental Temperature Distributions) fit the temperature difference curve well. The temperature between these Fundamental Temperature Distributions at a point (x, y, z) on the structure at any time  $t_o$  between  $t_1$  and  $t_2$  is then calculated by the following equation which is shown in *Figure* 6.0-2.

$$T_o(x,y,z,t_o) = T_1(x,y,z,t_1) + \frac{t_o - t_1}{t_2 - t_1} \big[ T_2(x,y,z,t_2) - T_1(x,y,z,t_1) \big]$$

In this way the stress computations require the input from disk of a very limited number of these Fundamental Temperature Distributions, thus drastically reducing the I/O and total execution time. The application of this method is further described in Section 7.0.

After the load steps have been selected, they are applied cyclically 4 times as shown in *Figure* 6.0-3.

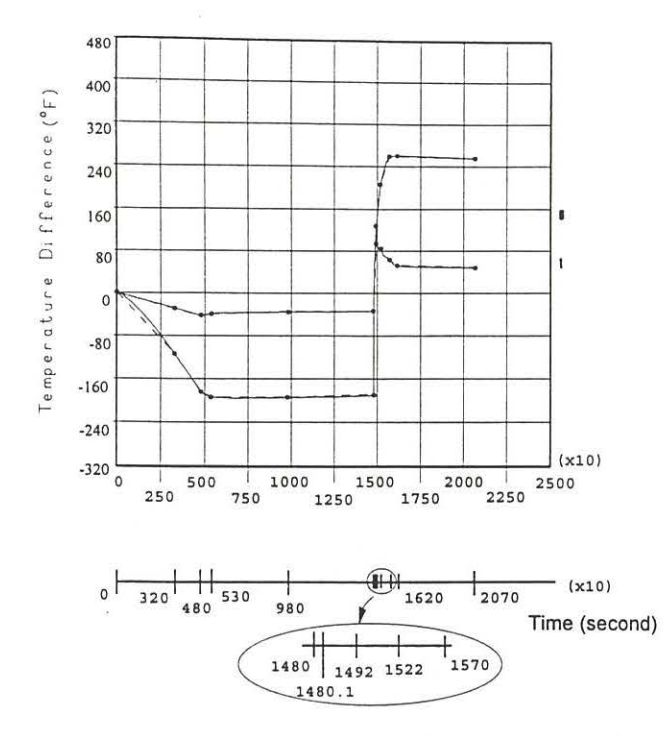


Figure 6.0-1: Load Steps Picked and Comparison of Linearized Temperature Difference Curves with the Original

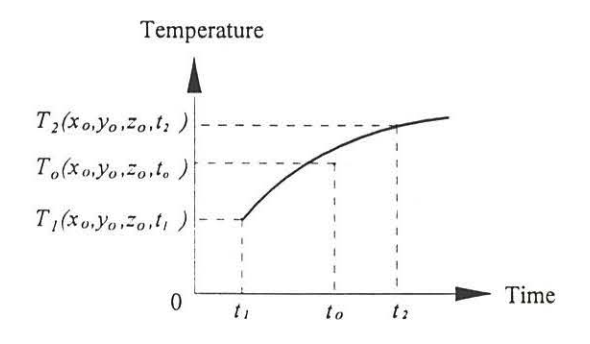


Figure 6.0-2: Linearization of Temperature

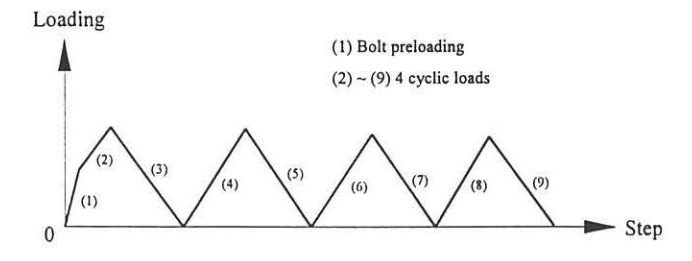


Figure 6.0-3: Cyclic Loads

#### 7.0 DISCUSSION OF ANALYSIS AND RESULTS

#### 7.1 Thermal Transient

The nodes around the access hole and the contact surface are selected to calculate the temperature difference. This is because the distortion in these regions is of primary concern. These nodes are plotted in *Figure 7.1-1*. For example *Figure 6.0-1* shows the temperature difference through the shell thickness and on the shell outer surface.

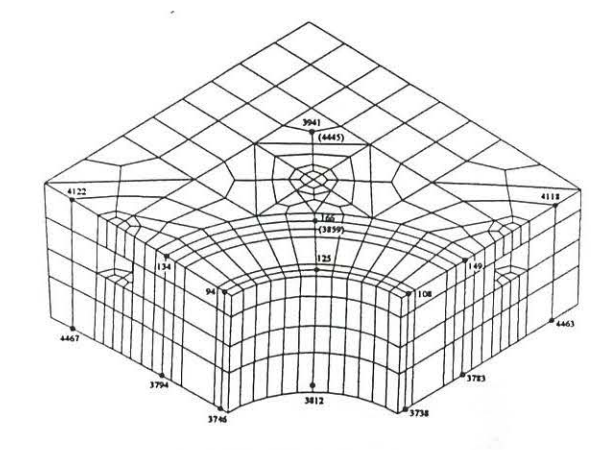


Figure 7.1-1: Nodes Picked to Calculate the Temperature Differences

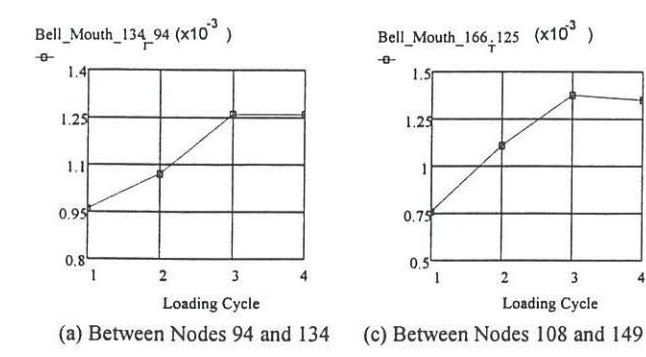
The input-deck load steps for elastic-plastic analysis are picked based on *Figure* 6.0-1. Since it is temperature differences that drive thermal strain, fundamental temperature distributions are selected at those time corresponding to the peak temperature difference and others between them as well. These points have been shown with symbol • in *Figure* 6.0-1.

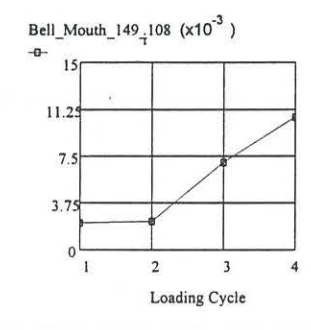
The predicted temperature distribution (during the structural run) were compared with the real temperature distribution from the thermal transient analysis in Ref. 3. A high degree of accuracy was demonstrated. Therefore, the combined effect of the thermal transient and the pressure loading can be handled in 'real-time' by calculating all temperature distributions between fundamental temperature distributions within the elastic-plastic stress computations.

### 7.2 Bell-mouthing of the Opening

The nodal displacements around the opening in the direction perpendicular to the contact surface are extracted to calculate the bell mouth shape. The results are plotted in *Figure* 7.2-1. Note that the bell mouth shape is inward, i.e. the nodes further away from the opening have larger displacements (for example, node 134 has a large displacement than node 94). This is because during the thermal transient, the opening has a lower temperature than the surrounding area. Although the internal pressure has a

tendency to cause the outward bell mouth shape, the effect is smaller than the thermal influence. Note that the distortions after four load cycles is not asymmptotic.





(b) Between nodes 125 and 166

Figure 7.2-1: Bell-mouth Displacement

#### 7.3 Variation of the Contact Pressure

To evaluate potential effects on leakage from the closure, it is important to examine the contact pressure between the contact surfaces. The contact pressures on each element when the bolts are tightened are plotted in *Figure* 7.3-1 where surface 1 and 2, element number and element line number are defined in *Figure* 7.3-2. Note that all the contact pressure of the contact elements are negative which means compression. There is no contact force on the surface 1 after bolt preload, hence the plot for surface 1 is not given. It is clear from *Figure* 7.3-1 that the contact force is uniformly distributed on each element line, but the magnitude is gradually decreased from outer to inner. This is because of the bending effect of the preloading on the cover. It should also be noted that because of symmetric boundary conditions, the contact force on the both edges (element 0 and 12) is about half of the others.

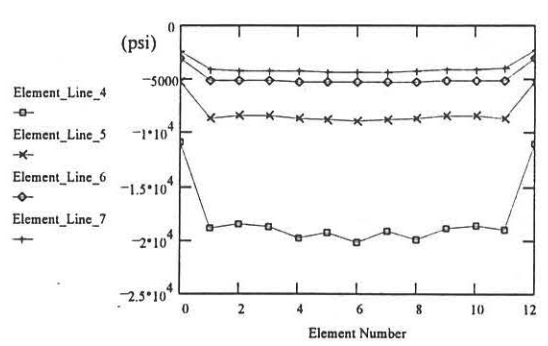


Figure 7.3-1: Contact Pressure on Surface 2 after Bolt Preloading

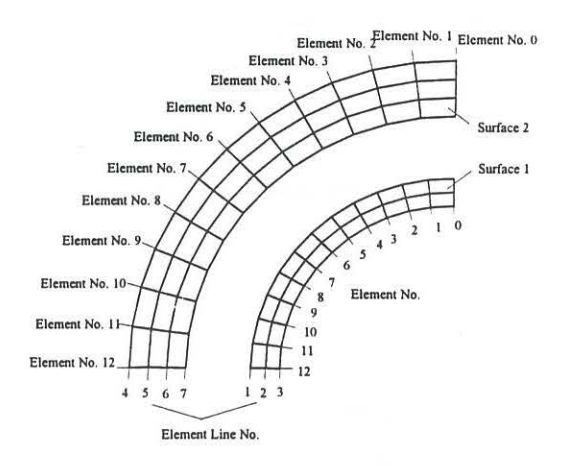
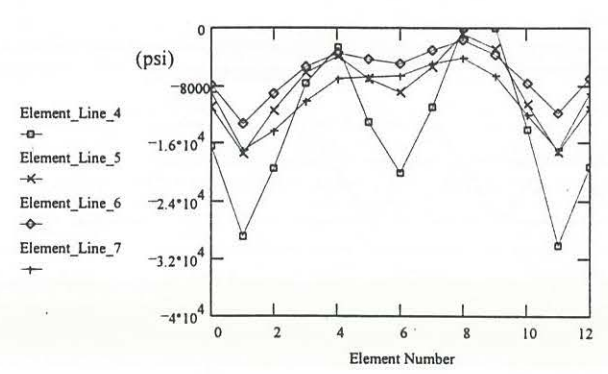
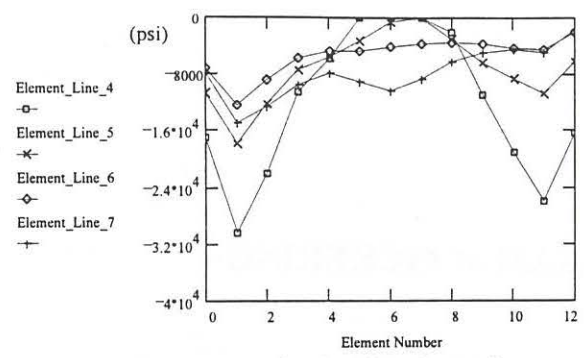


Figure 7.3-2: Definition of Surface, Element and Element Line Number

The variations of the contact pressures on the elements during the cyclic loadings are summarized in *Figure* 7.3-3. A more detailed result can be found in Ref. 3. In all the 4 transient cycles, it is found that the surface 1 is not in contact (hence the plots are not given). For surface 2, the middle of the most outside part (element Line 4) is lifted up (Element 7, 8 and 9). The contact pressure distributions become non-uniform.



(a) contact pressure after the 1st cycle transient



(b) contact pressureafter the 4th cycle transient

Figure 7.3-3: Variation of Contact Pressure on Surface 2 after Cyclic Loading

#### 8.0 CONCLUSIONS

The technique developed in this paper and that of Ref. 3 for handling the combined thermal transient and structural loading was proved to be a practical means of designing complex and highly stressed components. The technique makes it practical to carry out an inelastic analysis in "real time" with the combined effects of thermal and structural loading. The predicted temperature distribution calculated within the structural run has been shown to be very close to that of the distribution calculated in the thermal model.

It is concluded that after 4 cyclic loads, the structure has not shaken down and incremental distortion may continue in subsequent cyclic loading. Based on the first 4 cycle of warmup/rapid cooldown transient load, the bell-mouth shape of the present design is very small in the region of the contact surface area. Although a small portion of the cover was lifted up and the average contact pressure on the contact surface between the cover and the shell was decreased after each load cycle, there may be still sufficient pressure (contact force) to indicate no adverse effect on tightness leak.

#### 9.0 REFERENCES

- [1] ASME Boiler & Pressure Vessel Code, Section III, Division 1, Subsection NB and Appendices, No Addenda, 1986.
- [2] ANSYS User's Manual, Volume I, II and III, Rev. 5.2, August 31, 1995.
- [3] Elastic-Plastic Thermal Transient Stress Analysis of a Zero-Reinforcement Vessel Closure, G. McClellan, Y. Mou, PVP-Vol. 354, 111-119, 1997.